Australasian Physical & Engineering Sciences in Medicine (2019) 42:871–885
https://doi.org/10.1007/s13246-019-00773-2

TECHNICAL PAPER

Optimal b-values for diffusion kurtosis imaging in invasive ductal carcinoma versus ductal carcinoma in situ breast lesions

Filipa Borlinhas[1,2] · **Raquel C. Conceição**[1] · **Hugo A. Ferreira**[1]

Received: 15 November 2018 / Accepted: 27 June 2019 / Published online: 18 July 2019

Abstract

Diffusion kurtosis imaging (DKI) is a diffusion-weighted MRI technique that probes the non-Gaussian diffusion of water molecules within biological tissues. The purpose of this study was to investigate the DKI model optimal b-values combinations in invasive ductal carcinoma (IDC) versus ductal carcinoma in situ (DCIS) breast lesions. The study included 114 malignant breast lesions (64 IDC and 50 DCIS). Patients underwent a breast MRI examination which included a diffusion-weighted sequence (b = 0–3000 s/mm^2). For each lesion, the b-values were combined among each other (109 combinations) and each mean kurtosis (MK) parameter was obtained. Differences between the lesion groups and b-values combinations were assessed. Also, the diagnostic performance of the combinations was determined through receiver operating characteristic (ROC) curve analysis, and compared. Root mean square error (RMSE) was also obtained. All the b-values combinations showed significant differences between the lesion groups ($p < 0.05$). The combination 0, 50, 200, 750, 1000, 2000 s/mm^2 showed the best performance (AUC = 0.930, sensitivity = 95.3%, specificity = 82.0%, accuracy = 89.5%), with a RMSE of 17.65. The b-values combinations with the worst performance were composed of only high or ultra-high b-values, or with b = 1000 s/mm^2 as the maximum b-value. Better results were obtained when zero b-value was included in the DKI model fitting with at least one b-value below 1000 s/mm^2 and one b-value above 1000 s/mm^2 (conserving b = 1000 s/mm^2). Six was the optimal number of b-values, nonetheless other combinations with less b-values may be considered, but with a consequent diagnostic performance loss.

Keywords Diffusion · Diffusion kurtosis imaging (DKI) · b-values · Optimization · Breast cancer

Introduction

Diffusion kurtosis imaging (DKI) is a diffusion-weighted magnetic resonance imaging (MRI) technique that probes the non-Gaussian diffusion of water molecules within different tissue compartments [1–5]. The theory that has been put forward is that the DKI model may provide biological microstructural information on human tissues [1, 2], being sensitive to cell structures, intra or extra-cellular compartments, permeability, and other water diffusion phenomena [5, 6]. A wide range of investigational problems have been assessed with DKI, as well as anatomical regions and diseases [6–16], including breast cancer [17–24]. The multiplicity of studies is due to technology advances, which allow for the acquisition of data at ultra-high b-values (2000–5000 s/mm^2) [3], displaying non-Gaussian diffusion effects.

The literature indicates that the selection of the b-value range is extremely relevant for DKI studies, since they reflect the degree of diffusion weighting [25–27]. Different b-value ranges generate different estimations of DKI model parameters [28]. For instance, the maximum b-value is crucial for the DKI model fitting accuracy [1, 29]. In fact, the natural logarithmic signal intensity decay deviates from the monoexponential model curve when higher b-values are used [2], so it is accepted that a better DKI assessment is performed with these b-values [3, 15, 16, 28]. In this way,

✉ Filipa Borlinhas
filipaborlinhas@gmail.com

Raquel C. Conceição
raquelcruzconceicao@gmail.com

Hugo A. Ferreira
hugoferreira@campus.ul.pt

[1] Instituto de Biofísica e Engenharia Biomédica, Faculdade de Ciências, Universidade de Lisboa, Campo Grande, 1749-016 Lisbon, Portugal

[2] School of Health and Rehabilitation, Keele University, Staffordshire ST5 5BG, UK

the authors established a maximum b-value at 1500–2000 s/mm^2 for body studies [3]. The available studies in breast [17–24] use different b-values' ranges, number of b-values (4–8 b-values), and maximum (1000–3000 s/mm^2) and minimum b-values (0–50 s/mm^2). The variation is based on the need of weighting the use of low and high b-values. When using high b-values there is a decrease in accuracy and an increase in precision [1, 29]. When using lower b-values there is less differentiation between different tissue types [30]. Regarding the number of b-values of the diffusion-weighted sequence, it is considered that using more b-values increase the reliability of the DKI results and reduce the associated measurement errors and parameter uncertainties [4, 31–33]. Therefore, we hypothesise that a combination of b-values that includes more b-values will have better diagnostic performance, when compared to a combination with less b-values. The problem is that a large number of b-values translate into longer MRI scan times [3, 32], and potential motion artifacts, which discourage the usage of DKI in clinical practice.

The different results obtained in DKI studies show variability that may be due not only to tissue biology and structure, but also to the use of different b-values [29]. A few studies were developed in the brain [31, 33, 34] and prostate [35–37] exploring the b-values effect on the DKI model. Consequently, the development of clinical recommendations stipulating an adequate choice of b-values for specific suspected pathologies and tissue types should be prioritized [29]. This is a topic of current and active research due to its influence on the DKI model results.

The purpose of this study is to identify if different ranges of b-values may influence DKI model performance results. We hypothesise that different combinations of b-values can correspond to different diagnostic performance. Thus, we aim to isolate the best set of b-values in the differentiation of two common breast cancer histological types, the invasive ductal carcinoma (IDC) and the ductal carcinoma in situ (DCIS) lesions, based on a receiver operating characteristics (ROC) curve analysis. These groups of lesions were chosen because they are frequent malignant lesions, they may have different prognosis, axillary node evaluation, and different surgical approaches [38]. Also, its complete differentiation is a challenge for diffusion models. To the best of our knowledge, this is the first study that attempts to associate an optimal b-value combination for DKI model with breast tissue and lesions, based on the ROC curve performance analysis.

Materials and methods

Patients

The protocol of this prospective study was approved by the Institutional Review Board, and informed consent was obtained from all patients. From November 2016 to March 2017, seventy patients with one or more IDC and/or DCIS breast lesions confirmed by histology (biopsy in all the cases and surgical specimens in the majority of the cases) enrolled in this study. Women who had undergone breast surgery, chemotherapy, or radiotherapy, and women with breast implants, were excluded from the study. The inclusion criteria were: clinical indication for breast MRI; if the patient was premenopausal, MRI should be performed between the 7th and the 14th day of her menstrual cycles; if the biopsy was performed previously to MRI, at least seven days between biopsy and the MRI examination should be guaranteed to reduce the probability of haemorrhage or oedema interference.

MR image protocol

Patients were imaged on a 3T MRI scanner (*Ingenia*; Philips Medical Systems, Netherlands) with a dedicated 16-channel breast coil (*ds Breast 16chAdaptive,* Philips Medical Systems, Netherlands). The normal breast examination protocol (T2-weighted, diffusion-weighted b-values = 0, 1000 s/mm^2, dynamic contrast-enhanced T1-weighted sequences, all in the axial plane) was applied. An additional acquisition of a Spin-Echo Single-Shot Echo-Planar diffusion-weighted imaging sequence was acquired for analysis before contrast agent. This sequence was acquired in the axial plane with orthogonal diffusion gradient directions and 10 b-values: 0 (number of averages = 1), 15 (1), 30 (1), 50 (1), 200 (1), 750 (1), 1000 (2), 1500 (4), 2000 (6), 3000 (6) s/mm^2. The other parameters of the sequence were: repetition time/echo time = 2154/97 ms; field-of-view = 340 × 340 mm^2; matrix = 172 × 169; number of slices = 10; thickness = 3 mm; slice gap = 0 mm; number of excitations = 2, scan time ≈ 5 min. The 10 slices aimed to cover the target lesion and not the entire breast, because of time constraints and number of b-values.

Regions-of-interest

The additional diffusion-weighted images were revised on an image processing software (Osirix v.8.0.1, Pixmeo Sarl, Switzerland). The Regions-of-interest (ROI) were defined in consensus by two radiology researchers (with 7 and 10 years of experience in breast imaging). When possible,

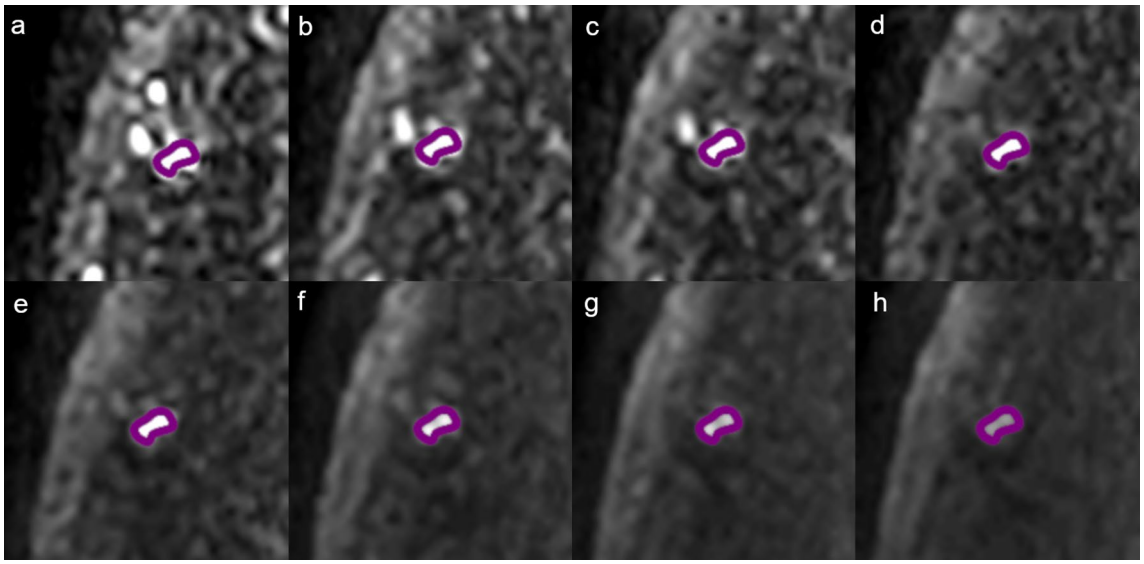

Fig. 1 Example of a Region-of-interest (ROI) definition in an invasive ductal carcinoma (IDC). The diffusion-weighted images **a**–**h** are from the same breast region, acquired with different b-values (0, 50, 200, 750, 1000, 1500, 2000, 3000 s/mm^2, respectively). It is possible to observe that in high b-value images, there is more contrast between the lesions (hyperintense) and the surrounding tissue, relatively to the images with low b-values

the ROIs were delimited on two contiguous representative regions of the lesion, with larger diameters and visibility, and the intensity signal was estimated through the means of both ROIs. Contours were defined on the viable limits of the hyperintense lesions with a diameter of at least 4 mm, on b = 3000 s/mm^2 images (Fig. 1). Necrotic, haemorrhage, and cystic areas were avoided. The ROIs were then copied to the same location onto other b-value images.

DKI model fitting

Thereafter, the respective mean intensity values of the ROIs were the input to an in-house developed Matlab software (R2015b, MathWorks Inc., US) script that fitted the DKI model through Eq. 1 [1–4]:

$$S_b/S_0 = \exp(-b \times MD + b^2 \times MD^2 \times MK/6) \quad (1)$$

the mean diffusivity (MD) parameter (mm^2/s) is determined by the slope of the signal intensity curve as the b-value approaches zero [3], and may be interpreted as the apparent diffusion coefficient for a non-Gaussian distribution [16]. The mean kurtosis (MK) parameter (no units) expresses the deviation of water diffusion profile from Gaussian probability distribution due to the natural structure of the biological tissues as, for example, cell membranes and intracellular components [2, 3]. S_b/S_0 is the overall signal attenuation, and b is the b-value (s/mm^2).

In this study, only the MK parameter was considered, since it showed higher diagnostic performance than the MD parameter in previous DKI model studies, when comparing benign and malignant lesions [24, 39]. 109 different b-values combinations were tested (see "Appendix"). Furthermore, the scan time and signal-to-noise ratio (SNR) was simulated on the MRI console and registered for the b-value combinations with the best performance. It was assured, for each b-value combination, that at least 3 b-values were selected, b = 15 and 30 s/mm^2 were excluded, and b = 1000 s/mm^2 was included in the range. The b-values of 15 and 30 s/mm^2 were acquired for use in another diffusion model analysis, not described herein. The b-value of 1000 s/mm^2 was used in this study for comparison with previous studies, and because it is a "transition" b-value between the lower and the higher b-values, being relevant to DKI fitting.

Statistical analysis

Using the statistics SPSS software (Release 25.0.0–2017, IBM, Armonk, NY) and suiting non-normal distribution of MK values, non-parametric statistical test Mann–Whitney U was used to assess IDC and DCIS groups' differences. This was performed for each b-value combination. Moreover, the Wilcoxon signed rank test was used for the comparison of two b-value combinations at a time, considering the distribution of MK values for the IDC and DCIS groups. In both statistical tests, a significance of 5% was considered. The root mean square error (RMSE) associated to the fitting was computed and compared among the different b-value combinations. The resulting MK parameters, for the different DKI model fits, were then compared in terms of lesion group differentiation performance with a ROC

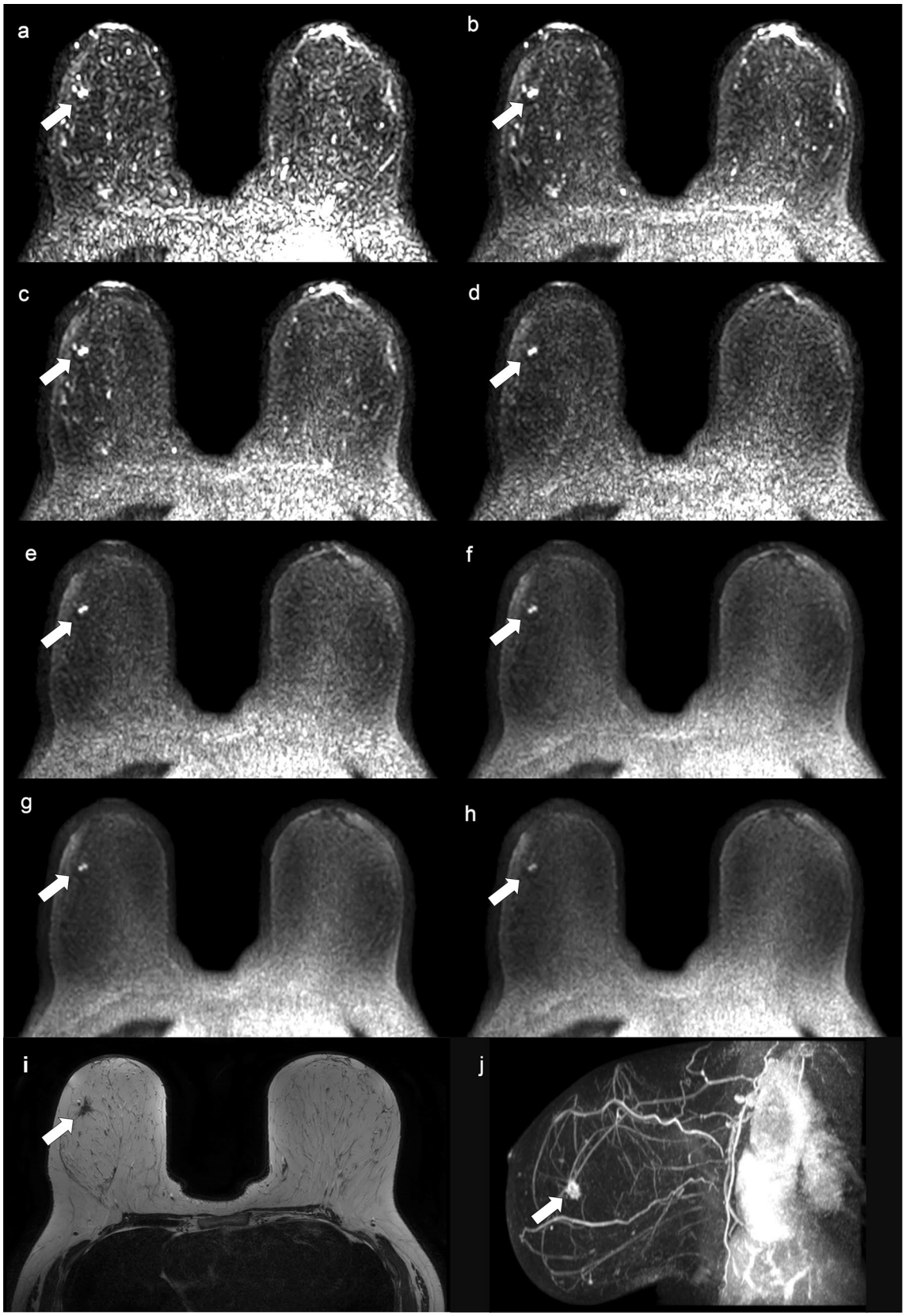
a
b
c
d
e
f
g
h
i
j

◂**Fig. 2** Invasive ductal carcinoma (IDC) in the right breast. Axial bilateral diffusion-weighted MR images (**a**–**h**) obtained at b = 0, 50, 200, 750, 1000, 1500, 2000, 3000 s/mm^2, respectively. It is possible to see that the lesions are best visualized at higher b-values because of higher contrast between the lesion and the breast parenchyma. Axial bilateral T2-weighted image (**i**) and a sagittal post contrast subtraction maximum intensity projection image of the affected breast (**j**)

curve analysis. The test was considered positive/negative when the diagnosis was IDC/DCIS, respectively, since it was assumed to be clinically worse to misclassify a DCIS as an IDC, than the opposite: DCIS lesions are believed to be a precursor of IDC lesions; generally, the DCIS lesions require shorter clear resection margins than an IDC; normally, axillary lymph node staging is not routinely recommended for patients with a non-operative diagnosis of DCIS alone [38]. The Area Under Curve (AUC) of the DKI fittings were compared with MedCalc (v. 15.0, Ostend, Belgium) using the DeLong et al. method [40]. To rank the ROC results of the different fittings, the first criteria were the sensitivity results, being sorted by its highest values. Then, the second criterion was the specificity, which was used to re-rank the b-values combinations, and then the accuracy and AUC were consider to solve draws between combinations rank. This procedure had the purpose to reduce the misclassified cases of IDC lesions, then to reduce misclassified cases of DCIS lesions, and to consider the global reliability and power of the DKI model in the differentiation of group of lesions. Finally, the combinations with a difference of more than 20% between sensitivity and specificity results were eliminated from the ranking. This procedure served as a filter of the b-values combinations to provide diagnostic acceptability in practice.

Results

Patients

Of the 70 patients who were first included in the study, 14 patients were excluded from the assessment due to image artifacts or poor image quality (number of patients—$n = 10$), and presence of haemorrhage or inflammation ($n = 4$). Thus, 56 patients (mean age 62 years; range from 32 to 88 years) with 114 lesions were considered (size ≤ 1 cm = 13 lesions; 1–2 cm = 44 lesions; > 2 cm = 57 lesions), 64 IDC and 50 DCIS lesions (Figs. 2, 3).

Differentiation between IDC and DCIS lesions

The IDC lesions showed significant lower MK values when compared to DCIS lesions ($p < 0.05$) (Table 1). This result was obtained for all the b-value combinations in study.

Combinations of b-values

The summarized performance results are presented in Table 2 and the complete results are showed in "Appendix". Considering the ranking, the best performance in IDC and DCIS lesions differentiation, was obtained for the following cases (Table 2): b = 0, 50, 200, 750, 1000, 2000 s/mm^2 (best combination); b = 0, 200, 750, 1000, 1500, 2000 s/mm^2; b = 0, 200, 750, 1000, 2000 s/mm^2; b = 0, 50, 750, 1000, 2000 s/mm^2; b = 0, 750, 1000, 2000 s/mm^2; b = 0, 50, 200, 750, 1000, 1500, 2000 s/mm^2 (no significant differences in the AUC, $p > 0.05$, and similar RMSE). The b = 0, 50, 200, 750, 1000, 2000 s/mm^2 and b = 0, 200, 750, 1000, 1500, 2000 s/mm^2 showed significant differences in the MK distribution, in both IDC and DCIS groups ($p < 0.001$, $p = 0.018$, respectively). Significant differences were also observed when comparing the other combinations with better performance with the combination with the best performance, except for b = 0, 200, 750, 1000, 2000 s/mm^2 (IDC—$p = 0.650$, DCIS—$p = 0.452$, respectively). The fittings were very similar for some of these combinations, as it shown in Fig. 4.

When considering the combination with all the b-values (b = 0, 50, 200, 750, 1000, 1500, 2000, 3000 s/mm^2) to the combination with the best performance, a non-significant decrease was observed in AUC (0.913 and 0.930, respectively), as well as a lower sensitivity (89.1% and 95.3%, respectively), specificity (80.0% and 82.0%, respectively), and accuracy (85.1% and 89.5%, respectively). These two combinations showed a similar RMSE (20.40, 17.65, respectively). In this case, significant differences were observed between the MK distribution in both IDC and DCIS groups ($p < 0.001$).

The best combination (b = 0, 50, 200, 750, 1000, 2000 s/mm^2) and b = 50, 200, 750, 1000, 2000 s/mm^2 where compared to study the relevance of the inclusion or exclusion of b = 0 s/mm^2. The combination with the b = 0 s/mm^2 showed higher sensitivity and accuracy, but lower specificity when compared to the combination which excludes b = 0 s/mm^2. Nonetheless, no significant differences were observed between the respective AUCs ($p < 0.05$), as well as their MK distributions (IDC—$p = 0.140$, DCIS—$p = 450$).

Comparing the combinations b = 0, 50, 200, 750, 1000, 2000 s/mm^2 and b = 0, 50, 200, 750, 1000, 2000, 3000 s/mm^2, or b = 0, 50, 200, 750, 1000, 2000 s/mm^2 and b = 0, 50, 200, 750, 1000, 3000 s/mm^2, it was possible to evaluate the maximum b-values of the combinations. In both comparisons, significant differences between the MK distributions were observed for both IDC and DCIS groups ($p < 0.001$), and no significant differences between AUC were observed ($p > 0.05$). The combination which ends with b = 2000 s/

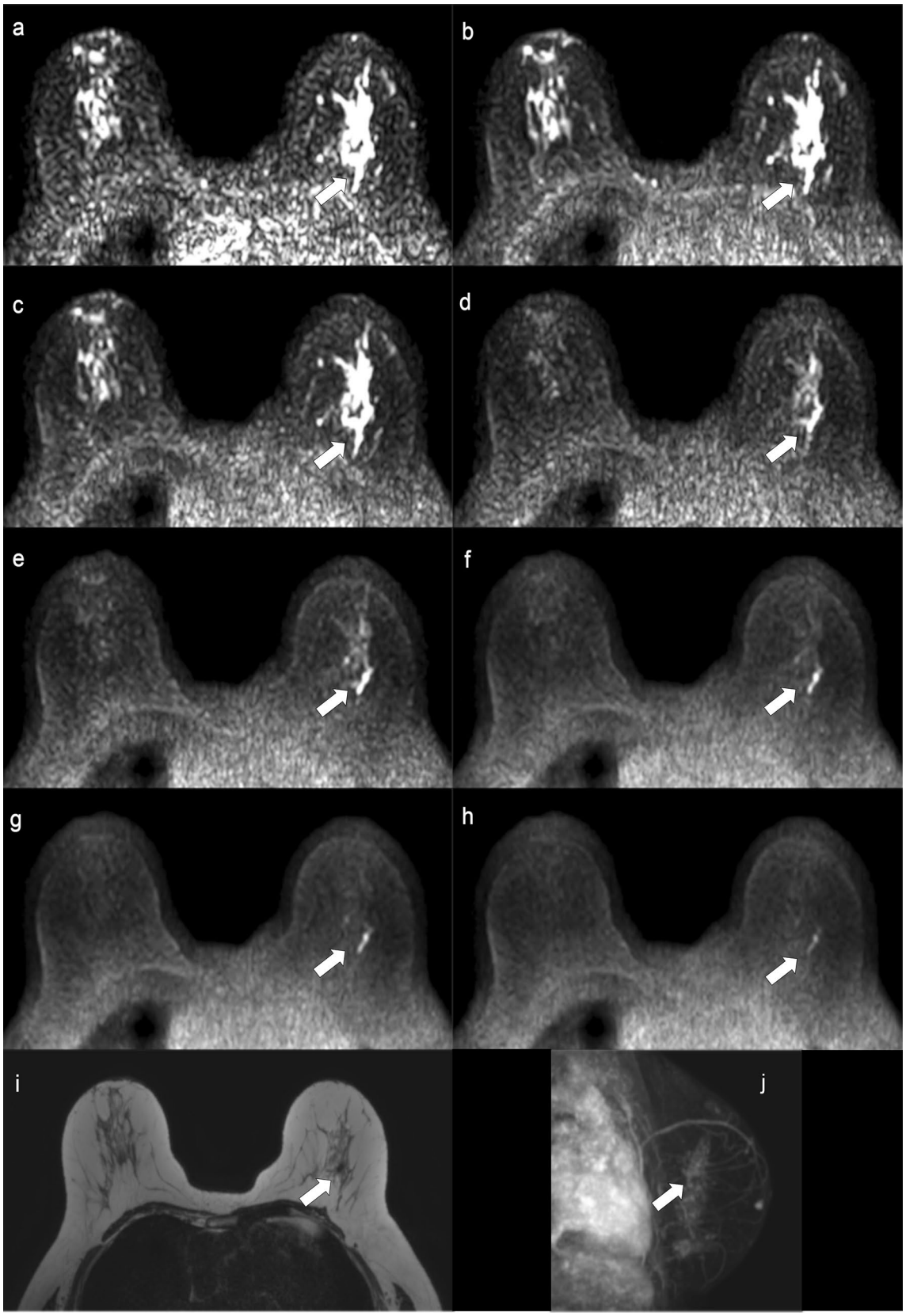

Fig. 3 Ductal carcinoma in situ (DCIS) in the left breast. Axial bilateral diffusion-weighted MR images (**a**–**h**) obtained at b = 0, 50, 200, 750, 1000, 1500, 2000, 3000 s/mm^2, respectively. Axial bilateral T2-weighted image (**i**) and a sagittal post contrast subtraction maximum intensity projection image of the affected breast (**j**)

Table 1 Example of the MK values obtained for the 10 best b-values combinations

Best b-values combinations	MK ± SD [Min;Max]		*p* value*
	IDC	DCIS	
0, 50, 200, 750, 1000, 2000	1.26 ± 0.21 [0.91;1.89]	0.86 ± 0.19 [0.42;1.23]	< 0.001
0, 200, 750, 1000, 1500, 2000	1.27 ± 0.21 [0.92;1.93]	0.85 ± 0.24 [− 0.17;1.24]	
0, 200, 750, 1000, 2000	1.23 ± 0.20 [0.91;1.90]	0.83 ± 0.24 [− 0.06;1.23]	
0, 50, 750, 1000, 2000	1.24 ± 0.22 [0.89;1.80]	0.85 ± 0.17 [0.58;1.20]	
0, 750, 1000, 2000	1.24 ± 0.22 [0.88;1.82]	0.85 ± 0.17 [0.51;1.19]	
0, 50, 200, 750, 1000, 1500, 2000	1.27 ± 0.21 [0.92;1.93]	0.87 ± 0.20 [0.35;1.23]	
50, 200, 750, 1000, 1500, 2000	1.26 ± 0.22 [0.91;1.92]	0.88 ± 0.18 [0.52;1.23]	
0, 1000, 2000	1.20 ± 0.27 [0.00;1.82]	0.85 ± 0.17 [0.52;1.17]	
0, 200, 1000, 2000	1.24 ± 0.21 [0.91;1.96]	0.82 ± 0.28 [1.24;1.52]	
0, 1000, 1500, 2000	1.22 ± 0.24 [0.57;1.82]	0.86 ± 0.17 [0.55;1.19]	

MK mean kurtosis, *SD* standard deviation, *Min* minimum, *Max* maximum, *IDC* invasive ductal carcinoma, *DCIS* ductal carcinoma in situ

*Mann–Whitney U test evaluating the differences between IDC and DCIS for each combination

mm^2 showed higher AUC, sensitivity, and accuracy, but equal specificity (0.930, 95.3%, 89.5%, and 82.0%, respectively) when compared to b = 0, 50, 200, 750, 1000, 2000, 3000 s/mm^2 (0.916, 87.5%, 85.1%, and 82.0%, respectively) and b = 0, 50, 200, 750, 1000, 3000 s/mm^2 (0.910, 87.5%, 85.1%, and 82.0%, respectively).

The combination b = 0, 1000, 2000 s/mm^2 showed no significant differences in AUC, when compared to the best combination ($p > 0.05$), but it showed lower sensitivity (92.2% and 95.3%, respectively) and accuracy (87.7% and 89.5%, respectively). Also, significant differences were found in the MK distributions of these two combinations ($p \leq 0.001$).

The worst combinations, with the lowest performance indicators, or unbalanced sensitivity and specificity, were: b = 1000, 1500, 2000 s/mm^2; b = 750, 1000, 1500 s/mm^2; b = 750, 1000, 2000 s/mm^2; b = 1000, 1500, 2000, 3000 s/mm^2 (Table 3). All these combinations showed significant differences in AUCs when compared to the best combination in the rank (b = 0, 50, 200, 750, 1000, 2000 s/mm^2). In Fig. 4 it is possible to observe some of these combinations fittings.

Scan time and SNR

The simulated scan times, for 10 slices, for these four b-values combinations ranged between 1 min and 55 s (b = 0, 750, 1000, 2000 s/mm^2) and 2 min and 55 s (b = 0, 200, 750, 1000, 1500, 2000 s/mm^2) (Table 1). The combination b = 0, 50, 200, 750, 1000, 2000 s/mm^2 had an acquisition time of 2 min and 19 s. Considering the combination b = 0, 1000, 2000 s/mm^2 the scan time was 1 min and 43 s. The SNR of the four best combinations ranged from 1.191 to 1.193, relatively to the baseline sequence.

Discussion

Every b-value combination showed significant differences in the differentiation between IDC and DCIS lesions, but different diagnostic performances were observed between these combinations. Based on the ROC curve analysis, the combination b = 0, 50, 200, 750, 1000, 2000 s/mm^2 was the one with the best sensitivity and accuracy, and with a good specificity and AUC, when compared to the other combinations. Similar diagnostic performances were also obtained for other combinations, with only minor variations in the included b-values. The RMSE associated to the fitting of the DKI model was similar for the best four b-value combinations. The combinations with the worst diagnostic performances only include higher b-values, or their maximum b-value is b = 1000 s/mm^2.

The inclusion of b = 0 s/mm^2 was always present in the 6 best b-values combinations. There are authors that do not include b = 0 s/mm^2 in the DKI fitting in order to reduce perfusion effects, and start with b = 50 or 250 s/mm^2 [3, 10, 18–20]. The relevance of the b = 0 s/mm^2 is stated in the literature as the baseline value [4], being acquired and used in the majority of relevant studies [4, 8, 11, 13–16, 29, 41].

The lower b-values also showed to be important in the DKI model, being included in some of the combinations with the better diagnostic performance in this study. Consistent with these findings, in a prostate tissue study, b-values lower than 200 s/mm^2 were used [35]. In disagreement with these findings, the literature suggests that probably the b-values below 400 s/mm^2 are dispensable and may create bias in the DKI model fitting considering perfusion effects [3].

The optimal maximum b-values combinations showed b = 2000 s/mm^2 to be the maximum b-value with better performance results, when compared to b = 3000 s/mm^2.

Table 2 Summary of the performance metrics and RMSE of the MK parameter using different b-values combination

Ranking position	b-values combinations (s/mm^2)	Cut-off value	AUC	SE	Asymptotic 95% CI	Sensitivity (%)	Specificity (%)	Accuracy (%)	RMSE
1st	0, 50, 200, 750, 1000, 2000	0.99	0.930	0.023	[0.885;0.976]	95.3	82.0	89.5	17.65
2nd	0, 200, 750, 1000, 1500, 2000	1.00	0.926	0.024	[0.878;0.973]	95.3	82.0	89.5	14.35
3rd	0, 200, 750, 1000, 2000	1.00	0.928	0.024	[0.882;0.974]	93.8	82.0	84.6	14.38
4th	0, 50, 750, 1000, 2000	0.98	0.932	0.023	[0.888;0.977]	92.2	84.0	88.6	13.18
5th	0, 750, 1000, 2000	0.97	0.931	0.023	[0.886;0.976]	92.2	84.0	88.5	5.52
6th	0, 50, 200, 750, 1000, 1500, 2000	1.01	0.927	0.024	[0.881;0.974]	92.2	82.0	87.7	17.15
7th	50, 200, 750, 1000, 1500, 2000	1.00	0.924	0.024	[0.877;0.971]	92.2	82.0	87.7	10.19
8th	0, 1000, 2000	0.96	0.912	0.028	[0.858;0.966]	92.2	82.0	87.7	0.79
…	…	…	…	…	…	…	…	…	…
14th	50, 200, 750, 1000, 2000	1.02	0.927	0.024	[0.880;0.973]	90.6	84.0	87.7	10.62
…	…	…	…	…	…	…	…	…	…
34th	0, 50, 200, 750, 1000, 1500, 2000, 3000	0.92	0.913	0.026	[0.861;0.964]	89.1	80.0	85.1	20.40
…	…	…	…	…	…	…	…	…	…
47th	0, 50, 200, 750, 1000, 2000, 3000	0.92	0.916	0.026	[0.865;0.967]	87.5	82.0	85.1	20.49
48th	0, 50, 200, 750, 1000, 3000	0.09	0.910	0.027	[0.857;0.962]	87.5	82.0	85.1	18.86
…	…	…	…	…	…	…	…	…	…
98th	50, 750, 1000	1.23	0.816	0.040	[0.737;0.895]	67.2	86.0	75.4	0.66
99th	0, 50, 200, 750, 1000	1.28	0.754	0.045	[0.665;0.843]	67.2	78.0	71.9	14.42
100th	0, 200, 750, 1000	1.26	0.744	0.046	[0.654;0.835]	67.2	78.0	71.9	9.00
101st	0, 200, 1000	1.26	0.728	0.048	[0.634;0.822]	67.2	78.0	71.9	1.07

AUC area under the curve, *SE* standard error, *CI* confidence interval, *RMSE* root mean square error

A previous study regarding the choice of the maximum b-value to use in the DKI model [42], showed a slight performance advantage of the b = 3000 s/mm^2 comparatively to b = 2000 s/mm^2. Nonetheless, and consistent with Chuhutin et al. [29] findings, the error of the fitting increased by replacing b = 2000/mm^2 with 3000 s/mm^2, indicating a strong dependency of the maximum b-value in fitting errors. These results may be attributed to lower SNR, associated to higher b-values [3, 8]. The formula $b \leq 3/DK$ (D—diffusion, K—kurtosis coefficient), is presented as a guide to the choice of the maximum b-value [1, 19]. Considering this formula, ultra-high b-values would have to be used, leading to increased estimation errors, due to DKI model prediction of increasing signal intensity as the b-value increases, [1, 3] and decreased sensitivity to subtle lesions [29]. When using high b-values, typically there is a longer application of the diffusion gradients, which is more suitable for the brain, characterised by an intrinsic longer T2 relaxation time [8]. In the case of the breast tissue, the T2 is shorter and the transverse relaxation will decay faster, so ultra-high b-values should not be applied.

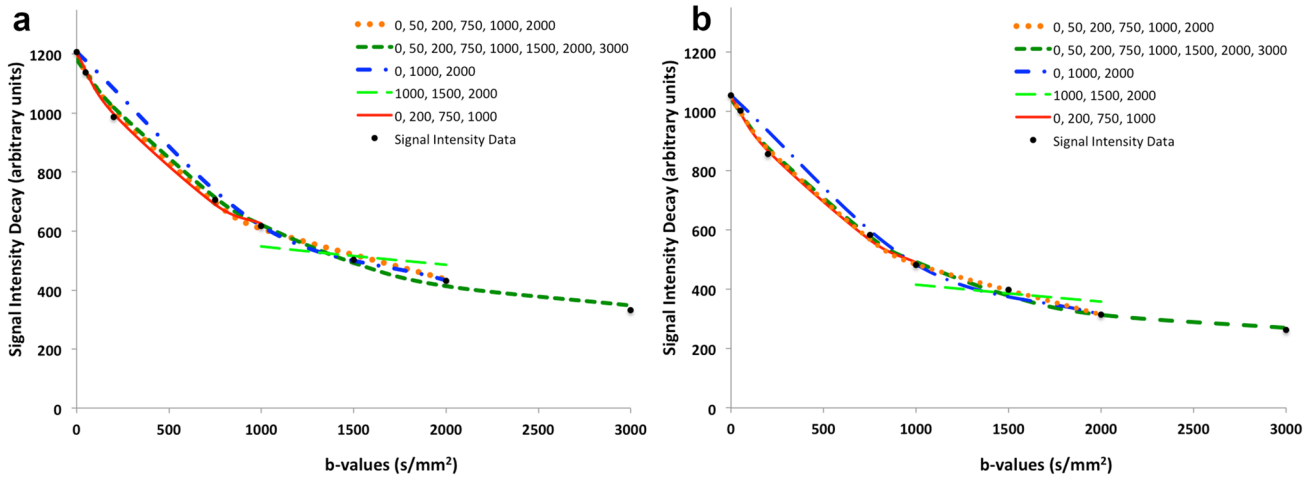

Fig. 4 Fitting plots of DKI model for an invasive ductal carcinoma (**a**), and for a ductal carcinoma in situ (**b**). The fittings correspond to different b-values combinations (s/mm^2)

Table 3 Combinations with the worst diagnostic performances or with severe unbalanced sensitivity and specificity

b-values combinations	Cut-off value	AUC	Asymptotic 95% CI	Sensitivity (%)	Specificity (%)	Accuracy (%)	RMSE
750, 1000, 1500[a]	− 169.35	0.590	[0.484;0.696]	100.0	16.0	62.5	65.48
1000, 1500, 2000, 3000[a]	0.91	0.815	[0.736;0.894]	95.3	62.0	80.7	14.67
1000, 1500, 3000[a]	0.92	0.799	[0.718;0.880]	85.9	62.0	75.4	12.91
0, 50, 200, 750, 1000[b]	1.28	0.754	[0.665;0.843]	67.2	78.0	71.9	14.42
0, 200, 750, 1000[b]	1.26	0.744	[0.654;0.835]	67.2	78.0	71.9	9.00
0, 200, 1000[b]	1.26	0.728	[0.634;0.822]	67.2	78.0	71.9	1.07
750, 1000, 1500, 2000[ab]	0.98	0.715	[0.620;0.809]	60.9	88.0	72.8	46.75
1000, 2000, 3000[ab]	1.08	0.660	[0.559;0.760]	56.3	82.0	67.5	49.49
0, 50, 1000[ab]	1.38	0.628	[0.523;0.733]	54.7	80.0	65.8	18.31
750, 1000, 2000[ab]	0.97	0.650	[0.550;0.750]	48.4	88.0	65.8	56.50
1000, 1500, 2000[ab]	0.37	0.589	[0.485;0.693]	14.1	98.0	50.9	72.10

[a]Combinations with a difference of more than 20% between sensitivity and specificity results

[b]Combinations with low sensitivity

AUC area under curve, *CI* confidence interva, *RMSE* root mean square error

Associated to the worst performances are the b-values combinations composed only by high or ultra-high b-values, or when the maximum b-value is 1000 s/mm^2. The b-values combination 0, 200, 750, 1000 s/mm^2 shows good fitting to the data, nonetheless this was a combination with lower diagnostic performance. There is a deviation from the monoexponential decay curve in b-values higher than b = 1000 s/mm^2, and DKI model assesses this behavior. Consequently, if these high b-values are not included in the combination, the diagnostic performance with DKI will be low. The generic ideal situation in body studies reported by Rosenkrantz et al. have considered 5 b-values: 2 b-values below 1000 s/mm^2 and higher than 200 s/mm^2, the 1000 s/mm^2 itself, and 2 ultra-high b-values. In the present study the optimal combination had 6 b-values, but others with less b-values also showed good results in terms of diagnostic performance: a single b-value above 1000 s/mm^2 is enough, preferably b = 2000 s/mm^2; and at least one b-value below 1000 s/mm^2. The use of 3 b-values in the present study, consistently with DKI brain studies of Yan et al. and Fukunaga et al. [4, 31], is a valid combination, as it is showed by the ROC curve results of b = 0, 1000, 2000 s/mm^2. This combination is also in agreement with the 3 b-values minimum for probing the non-Gaussian phenomenon [3, 4, 6], and with a maximum b-value between 1500 and 2000 s/mm^2, presented by Li et al. [11]. The RMSE associated to b = 0, 1000, 2000 s/mm^2 was lower than the one obtained for the best b-value combination in the rank. This difference in the RMSE could be based on the inclusion of additional low b-values (≤ 100 s/mm^2) in

the model, which introduces an additional source of noise [32]. Of course, there is a loss of diagnostic performance, when compared to the combination with the best performance, but this choice also has to be weighted according to the available scan time. The 3 b-values combination has a shorter scan time than the best combination, because of the lower number of b-values [4]. The difference was 36 s because these are low b-values that take less time to acquire, and in this study only 10 slices were acquired just to cover the lesion. The optimal b-value range for the DKI model analysis on the breast will necessarily vary with many factors, such as: expected image noise and image quality; available time to apply the diffusion-weighted sequence; scanner hardware configuration and magnetic field; need to simultaneously apply other quantitative models [3]; the purpose of examination (staging, diagnosis, monitor therapeutics); and patient tolerance to the examination.

The combination with all the b-values in study did not show significant differences in the AUC, when compared to the best combination, but it showed a lower sensitivity, specificity, and accuracy. One possible explanation for these findings is the nature of the DKI model itself. The DKI model is only a mathematical representation of the real signal intensity data, which has limitations. Another possible justification is that the combinations without b = 1500 and 3000 s/mm^2 may be more suitable in the differentiation of the IDC and DCIs groups of lesions specifically. In agreement with this, at higher b-values the quadratic behaviour of the DKI model function will no longer be valid, meaning that it will not reflect the signal intensity data [43, 44].

A limitation of the study was the type of lesions under evaluation. The obtained results are valid for the differentiation of these two types of malignant lesions and may be different when other types of lesions are compared. In the future, this optimal b-value combination should also be applied and assessed in normal breast tissue and other types of breast lesions. The low b-values inclusion in the best combinations was relevant for their diagnostic performance, and consequently this should be related to perfusion MRI data in the future. Another limitation was the absence of MD performance results in the same conditions as the MK parameter. In future studies, the MD diagnostic performance should also be analysed individually and in conjunction with the MK parameter to assess possible advantages. Also, only one scanner was included in the study, so in the subsequent studies the results from other scanners of different vendors should be compared.

Conclusion

The present study shows that the choice of the b-values range affects the MK parameter estimation and its performance in the differentiation of IDC and DCIS lesions in the breast. A comparative analysis of the diagnostic performance of different b-value combinations, showed better results when the following were included in the DKI model fitting (conserving b = 1000 s/mm^2): b = 0 s/mm^2, at least one non-zero b-value below 1000 s/mm^2 and one b-value above 1000 s/mm^2. Six was the optimal number of b-values (0, 50, 200, 750, 1000, 2000 s/mm^2), nonetheless other combinations with less b-values may be considered, but with a consequent loss in the diagnostic performance. The use of an optimal b-value selected range may be an encouragement for DKI model implementation, as the total scan time becomes acceptable for clinical practice.

Acknowledgements This paper is supported by Fundação para a Ciência e a Tecnologia – FCT / MEC (PIDDAC) – under the Strategic Programme UID/BIO/00645/2013. The authors thank the participants of this study, and the Radiology Department staff of Instituto Português de Oncologia de Lisboa Francisco Gentil, E.P.E., Lisboa, Portugal, involved in this study. The authors also thank Nuno Loução for assistance with the MRI sequence.

Compliance with ethical standards

Conflicts of interest The authors declare that they have no conflict of interest.

Ethical approval All procedures performed in studies involving human participants were in accordance with the ethical standards of the institutional and/or national research committee and with the 1964 Helsinki declaration and its later amendments or comparable ethical standards. This article does not contain any studies with animals performed by any of the authors.

Informed consent Informed consent was obtained from all individual participants included in the study.

Appendix

See Table 4.

Table 4 Complete ROC curve results for each of the 109 b-values combination in test

b-values combinations (s/mm^2)	Cut-off value	AUC	Standard Error	Asymptotic 95% CI	Sensitivity (%)	Specificity (%)	Accuracy (%)	RMSE
0, 50, 200, 750, 1000, 2000	0.99	0.930	0.023	[0.885;0.976]	95.3	82.0	89.5	17.65
0, 200, 750, 1000, 1500, 2000	1.00	0.926	0.024	[0.878;0.973]	95.3	82.0	89.5	14.35
0, 200, 750, 1000, 2000	1.00	0.928	0.024	[0.882;0.974]	93.8	82.0	84.6	14.38
0, 50, 750, 1000, 2000	0.98	0.932	0.023	[0.888;0.977]	92.2	84.0	88.6	13.18
0, 750, 1000, 2000	0.97	0.931	0.023	[0.886;0.976]	92.2	84.0	88.5	5.52
0, 50, 200, 750, 1000, 1500, 2000	1.01	0.927	0.024	[0.881;0.974]	92.2	82.0	87.7	17.15
50, 200, 750, 1000, 1500, 2000	1.00	0.924	0.024	[0.877;0.971]	92.2	82.0	87.7	10.19
0, 1000, 2000	0.96	0.912	0.028	[0.858;0.966]	92.2	82.0	87.7	0.79
0, 200, 1000, 2000	0.99	0.909	0.028	[0.855;0.964]	92.2	80.0	86.8	13.19
0, 1000, 1500, 2000	0.97	0.908	0.028	[0.852;0.963]	92.2	80.0	86.8	4.95
50, 1000, 1500, 2000	0.97	0.906	0.028	[0.851;0.961]	92.2	80.0	86.8	4.85
0, 750, 1000, 1500	1.02	0.881	0.033	[0.816;0.946]	92.2	76.0	85.1	5.15
50, 750, 1000, 2000	1.01	0.929	0.023	[0.884;0.974]	90.6	84.0	87.7	5.39
50, 200, 750, 1000, 2000	1.02	0.927	0.024	[0.880;0.973]	90.6	84.0	87.7	10.62
50, 1000, 2000	0.97	0.910	0.028	[0.856;0.964]	90.6	82.0	86.8	0.73
50, 200, 1000, 2000	1.00	0.908	0.028	[0.852;0.963]	90.6	80.0	86.0	9.39
0, 50, 200, 1000, 1500, 2000	1.005	0.908	0.027	[0.854;0.962]	90.6	80.0	86.0	17.21
0, 50, 1000, 2000, 3000	0.90	0.907	0.028	[0.853;0.961]	90.6	80.0	86.0	16.99
0, 50, 1000, 1500, 2000, 3000	0.90	0.904	0.028	[0.848;0.959]	90.6	78.0	85.1	16.66
0, 50, 750, 1000, 1500	1.03	0.879	0.033	[0.815;0.943]	90.6	76.0	84.2	14.13
200, 750, 1000, 2000	1.01	0.913	0.027	[0.861;0.965]	89.1	84.0	87.7	5.37
0, 750, 1000, 1500, 2000	1.01	0.929	0.024	[0.883;0.976	89.1	84.0	86.8	7.54
0, 50, 750, 1000, 1500, 2000	1.02	0.928	0.023	[0.882;0.974]	89.1	84.0	86.8	14.33
50, 750, 1000, 1500, 2000	1.02	0.927	0.023	[0.881;0.973]	89.1	84.0	86.8	7.17
0, 50, 1000, 2000	0.98	0.916	0.027	[0.864;0.969]	89.1	84.0	86.8	13.79
50, 200, 750, 1000, 2000, 3000	0.92	0.910	0.027	[0.857;0.963]	89.1	84.0	86.0	14.81
0, 200, 750, 1000, 1500, 2000, 3000	0.92	0.911	0.027	[0.859;0.963]	89.1	82.0	86.0	18.56
0, 50, 750, 1000, 2000, 3000	0.91	0.910	0.027	[0.857;0.963]	89.1	82.0	86.0	17.69
50, 750, 1000, 2000, 3000	0.91	0.910	0.027	[0.857;0.963]	89.1	82.0	86.0	11.81
0, 50, 750, 1000, 1500, 2000, 3000	0.91	0.908	0.027	[0.855;0.961]	89.1	82.0	86.0	17.67
0, 750, 1000, 2000, 3000	0.90	0.908	0.027	[0.855;0.961]	89.1	82.0	86.0	12.24
0, 750, 1000, 1500, 2000, 3000	0.90	0.907	0.027	[0.853;0.960]	89.1	82.0	86.0	13.10
200, 750, 1000, 3000	0.91	0.896	0.030	[0.837;0.955]	89.1	82.0	86.0	5.78
0, 50, 200, 750, 1000, 1500, 2000, 3000	0.92	0.913	0.026	[0.861;0.964]	89.1	80.0	85.1	20.40
0, 200, 1000, 1500, 2000	1.01	0.908	0.027	[0.854;0.961]	89.1	80.0	85.1	13.85
0, 50, 750, 1000, 1500, 3000	0.90	0.903	0.028	[0.848;0.959]	89.1	80.0	85.1	16.69
0, 200, 750, 1000, 1500, 3000	0.90	0.907	0.027	[0.854;0.960]	89.1	78.0	84.2	17.78

Table 4 (continued)

b-values combinations (s/mm^2)	Cut-off value	AUC	Standard Error	Asymptotic 95% CI	Sensitivity (%)	Specificity (%)	Accuracy (%)	RMSE
0, 200, 1000, 1500, 3000	0.90	0.907	0.027	[0.854;0.961]	89.1	78.0	84.2	17.61
50, 200, 1000, 3000	0.90	0.904	0.028	[0.849;0.959]	89.1	78.0	84.2	10.79
50, 1000, 3000	0.89	0.902	0.029	[0.846;0.958]	89.1	78.0	84.2	0.88
0, 1000, 3000	0.88	0.899	0.029	[0.843;0.956]	89.1	78.0	84.2	0.86
750, 1000, 1500, 3000	0.92	0.835	0.038	[0.760;0.911]	89.1	74.0	82.5	20.07
750, 1000, 2000, 3000	0.90	0.830	0.039	[0.754;0.907]	89.1	72.0	82.5	22.24
0, 200, 750, 1000, 2000, 3000	0.92	0.916	0.026	[0.865;0.967]	87.5	84.0	86.0	18.39
200, 750, 1000, 1500, 2000	1.01	0.910	0.027	[0.857;0.963]	87.5	84.0	86.0	6.87
50, 200, 1000, 2000, 3000	0.92	0.908	0.028	[0.854;0.962]	87.5	84.0	86.0	14.22
0, 50, 200, 750, 1000, 2000, 3000	0.92	0.916	0.026	[0.865;0.967]	87.5	82.0	85.1	20.49
0, 50, 200, 750, 1000, 3000	0.90	0.910	0.027	[0.857;0.962]	87.5	82.0	85.1	18.86
0, 50, 1000, 1500, 2000	0.99	0.909	0.028	[0.855;0.964]	87.5	82.0	85.1	14.04
200, 750, 1000, 2000, 3000	0.93	0.902	0.029	[0.845;0.959]	87.5	82.0	85.1	10.48
0, 200, 1000, 2000, 3000	0.91	0.913	0.026	[0.862;0.965]	87.5	80.0	84.2	18.17
0, 200, 1000, 3000	0.89	0.911	0.026	[0.859:0,963]	87.5	80.0	84.2	15.22
50, 750, 1000, 1500, 2000, 3000	0.92	0.908	0.027	[0.855;0.961]	87.5	80.0	84.2	12.52
50, 200, 1000, 1500, 2000	1.02	0.901	0.029	[0.844;0.958]	87.5	80.0	84.2	10.43
200, 750, 1000, 1500, 2000, 3000	0.93	0.900	0.029	[0.843;0.957]	87.5	80.0	83.3	10.97
0, 750, 1000, 1500, 3000	0.91	0.908	0.027	[0.855;0.961]	87.5	78.0	83.3	18.96
50, 200, 1000, 1500, 2000, 3000	0.92	0.902	0.028	[0.8460.957]	87.5	78.0	83.3	14.38
0, 50, 750, 1000, 3000	0.90	0.905	0.028	[0.850;0.960]	85.9	84.0	85.1	14.99
0, 1000, 1500, 2000, 3000	0.90	0.900	0.029	[0.844;0.957]	85.9	82.0	85.1	10.44
50, 750, 1000, 3000	0.90	0.906	0.028	[0.851;0.960]	85.9	82.0	84.2	25.68
50, 200, 750, 1000, 1500, 2000, 3000	0.93	0.906	0.027	[0.852;0.960]	85.9	80.0	83.3	15.10
50, 1000, 1500, 2000, 3000	0.91	0.903	0.028	[0.848;0.959]	85.9	80.0	83.3	10.08
50, 1000, 2000, 3000	0.92	0.906	0.028	[0.852;0.961]	84.4	84.0	84.2	9.41
0, 750, 1000, 3000	0.89	0.902	0.028	[0.846;0.957]	84.4	82.0	83.3	6.38
0, 1000, 2000, 3000	0.90	0.901	0.029	[0.845;0.957]	84.4	82.0	83.3	9.73
200, 750, 1000, 1500, 3000	0.92	0.894	0.030	[0.835;0.953]	84.4	80.0	82.5	9.14
0, 200, 1000, 1500, 2000, 3000	0.93	0.910	0.027	[0.858;0.963]	82.8	82.0	82.5	18.29
50, 200, 750, 1000, 3000	0.91	0.905	0.028	[0.851;0.960]	82.8	84.0	83.3	11.87
0, 50, 1000, 3000	0.90	0.903	0.028	[0.847;0.959]	82.8	84.0	83.3	14.19
50, 200, 750, 1000, 1500	1.13	0.883	0.032	[0.821;0.946]	82.8	84.0	83.3	9.72
0, 50, 200, 750, 1000, 1500, 3000	0.92	0.908	0.027	[0.855;0.961]	82.8	82.0	82.5	19.96
50, 1000, 1500, 3000	0.91	0.900	0.029	[0.844;0.956]	82.8	82.0	82.5	7.15
0, 1000, 1500, 3000	0.90	0.897	0.029	[0.840;0.955]	82.8	82.0	82.5	8.67
0, 1000, 1500	1.01	0.855	0.037	[0.783;0.928]	82.8	80.0	81.6	0.79
0, 200, 750, 1000, 3000	0.93	0.910	0.027	[0.858;0.963]	81.3	86.0	83.3	16.02

Table 4 (continued)

b-values combinations (s/mm^2)	Cut-off value	AUC	Standard Error	Asymptotic 95% CI	Sensitivity (%)	Specificity (%)	Accuracy (%)	RMSE
50, 750, 1000, 1500, 3000	0.93	0.904	0.028	[0.849;0.959]	81.3	84.0	82.5	10.41
50, 200, 750, 1000, 1500, 3000	0.93	0.903	0.028	[0.849;0.958]	81.3	84.0	82.5	13.99
0, 50, 1000, 1500, 3000	0.93	0.900	0.029	[0.844;0.957]	81.3	84.0	82.5	15.83
200, 750, 1000, 1500	1.04	0.854	0.036	[0.782;0.925]	81.3	76.0	78.9	5.09
0, 50, 1000, 1500	1.03	0.829	0.039	[0.753;0.905]	81.3	74.0	78.1	13.60
750, 1000, 1500, 2000, 3000	0.91	0.804	0.041	[0.724;0.885]	81.3	74.0	78.1	28.64
750, 1000, 3000	0.91	0.793	0.044	[0.707;0.879]	81.3	72.0	77.2	7.61
0, 50, 200, 1000, 1500, 2000, 3000	0.96	0.910	0.027	[0.857;0.962]	79.7	86.0	82.5	20.46
50, 200, 1000, 1500, 3000	0.93	0.900	0.029	[0.845;0.956]	79.7	84.0	81.6	13.34
50, 750, 1000, 1500	1.10	0.880	0.032	[0.817;0.943]	79.7	84.0	81.6	5.04
50, 200, 1000, 1500	1.15	0.874	0.034	[0.808;0.940]	79.7	84.0	81.6	8.08
50, 200, 750, 1000	1.21	0.811	0.041	[0.730;0.892]	79.7	76.0	78.1	6.90
0, 200, 1000, 1500	1.10	0.807	0.041	[0.726;0.888]	79.7	74.0	77.2	10.82
0, 50, 200, 750, 1000, 1500	1.17	0.865	0.034	[0.798;0.932]	78.1	84.0	80.7	16.57
0, 200, 750, 1000, 1500	1.16	0.854	0.036	[0.784;0.924]	78.1	84.0	80.7	12.99
50, 200, 1000	1.22	0.790	0.044	[0.704;0.875]	78.1	76.0	77.2	0.52
50, 1000, 1500	1.08	0.842	0.038	[0.768;0.916]	75.0	84.0	78.9	0.87
0, 50, 200, 1000, 1500	1.15	0.816	0.040	[0.738;0.894]	75.0	78.0	76.3	340.73
0, 750, 1000	1.12	0.810	0.041	[0.730;0.891]	73.4	76.0	74.6	1.03
200, 750, 1000	1.10	0.766	0.045	[0.679;0.854]	68.8	76.0	71.9	0.79
0, 50, 750, 1000	1.20	0.755	0.045	[0.667;0.843]	68.8	76.0	71.9	11.53
0, 50, 200, 1000	1.26	0.732	0.048	[0.638;0.825]	68.8	76.0	71.9	12.36
50, 750, 1000	1.23	0.816	0.040	[0.737;0.895]	67.2	86.0	75.4	0.66
0, 50, 200, 750, 1000	1.28	0.754	0.045	[0.665;0.843]	67.2	78.0	71.9	14.42
0, 200, 750, 1000	1.26	0.744	0.046	[0.654;0.835]	67.2	78.0	71.9	9.00
0, 200, 1000	1.26	0.728	0.048	[0.634;0.822]	67.2	78.0	71.9	1.07
750, 1000, 1500, 2000	0.98	0.715	0.048	[0.620;0.809]	60.9	88.0	72.8	46.75
1000, 2000, 3000	1.08	0.660	0.051	[0.559;0.760]	56.3	82.0	67.5	49.49
0, 50, 1000	1.38	0.628	0.053	[0.523;0.733]	54.7	80.0	65.8	18.31
750, 1000, 2000	0.97	0.650	0.051	[0.550;0.750]	48.4	88.0	65.8	56.50
1000, 1500, 2000	0.37	0.589	0.053	[0.485;0.693]	14.1	98.0	50.9	72.10
750, 1000, 1500	− 169.35	0.590	0.054	[0.484;0.696]	100.0	16.0	62.5	65.48
1000, 1500, 2000, 3000	0.91	0.815	0.040	[0.736;0.894]	95.3	62.0	80.7	14.67
1000, 1500, 3000	0.92	0.799	0.041	[0.718;0.880]	85.9	62.0	75.4	12.91

AUC area under the curve, *CI* confidence interval, *RMSE* root mean square error

References

1. Jensen JH, Helpern JA (2010) MRI quantification of non-Gaussian water diffusion by kurtosis analysis. NMR Biomed 23:698–710. https://doi.org/10.1002/nbm.1518
2. Jensen JH, Helpern JA, Ramani A et al (2005) Diffusional kurtosis imaging: the quantification of non-gaussian water diffusion by means of magnetic resonance imaging. Magn Reson Med 53:1432–1440. https://doi.org/10.1002/mrm.20508
3. Rosenkrantz AB, Padhani AR, Chenevert TL et al (2015) Body diffusion kurtosis imaging: basic principles, applications, and considerations for clinical practice. J Magn Reson Imaging 42:1190–1202. https://doi.org/10.1002/jmri.24985
4. Yan X, Zhou M, Ying L et al (2013) Evaluation of optimized b-value sampling schemas for diffusion kurtosis imaging with an application to stroke patient data. Comput Med Imaging Graph 37:272–280. https://doi.org/10.1016/j.compmedimag.2013.04.007

5. Yablonskiy DA, Sukstanskii AL (2010) Theoretical models of the diffusion weighted MR signal. NMR Biomed 23:661–681. https://doi.org/10.1002/nbm.1520
6. Wu EX, Cheung MM (2010) MR diffusion kurtosis imaging for neural tissue characterization. NMR Biomed 23:836–848. https://doi.org/10.1002/nbm.1506
7. Goshima S, Kanematsu M, Noda Y et al (2015) Diffusion kurtosis imaging to assess response to treatment in hypervascular hepatocellular carcinoma. Am J Roentgenol 204:W543–W549. https://doi.org/10.2214/AJR.14.13235
8. Filli L, Wurnig M, Nanz D et al (2014) Whole-body diffusion kurtosis imaging. Invest Radiol 49:773–778. https://doi.org/10.1097/RLI.0000000000000082
9. Marrale M, Collura G, Brai M et al (2016) Physics, techniques and review of neuroradiological applications of diffusion kurtosis imaging (DKI). Clin Neuroradiol 26:391–403. https://doi.org/10.1007/s00062-015-0469-9
10. Budjan J, Sauter EA, Zoellner FG et al (2018) Diffusion kurtosis imaging of the liver at 3 Tesla: in vivo comparison to standard diffusion-weighted imaging. Acta radiol 59:18–25. https://doi.org/10.1177/0284185117706608
11. Li HM, Zhao SH, Qiang JW et al (2017) Diffusion kurtosis imaging for differentiating borderline from malignant epithelial ovarian tumors: a correlation with Ki-67 expression. J Magn Reson Imaging 46:1499–1506. https://doi.org/10.1002/jmri.25696
12. Rosenkrantz AB, Sigmund EE, Johnson G et al (2012) Prostate cancer: feasibility and preliminary experience of a diffusional kurtosis model for detection and assessment of aggressiveness of peripheral zone cancer. Radiology 264:126–135. https://doi.org/10.1148/radiol.12112290
13. Pentang G, Lanzman RS, Heusch P et al (2014) Diffusion kurtosis imaging of the human kidney: a feasibility study. Magn Reson Imaging 32:413–420. https://doi.org/10.1016/j.mri.2014.01.006
14. Suo S, Chen X, Ji X et al (2015) Investigation of the non-gaussian water diffusion properties in bladder cancer using diffusion kurtosis imaging: a preliminary study. J Comput Assist Tomogr 39:281–285. https://doi.org/10.1097/.0000000000000197
15. Cui Y, Yang X, Du X et al (2017) Whole-tumour diffusion kurtosis MR imaging histogram analysis of rectal adenocarcinoma: Correlation with clinical pathologic prognostic factors. Eur Radiol. https://doi.org/10.1007/s00330-017-5094-3
16. Huang L, Li X, Huang S et al (2017) Diffusion kurtosis MRI versus conventional diffusion-weighted imaging for evaluating inflammatory activity in Crohn's disease. J Magn Reson Imaging. https://doi.org/10.1002/jmri.25768
17. Borlinhas F, Lacerda L, Andrade A, Ferreira HA (2012) Diffusional kurtosis as a biomarker of breast tumors—C-1369. European Congress of Radiology. European Society of Radiology, Wien, Austria, pp 1–20. https://doi.org/10.1594/ecr2012/C-1369
18. Borlinhas F (2012) Quantificação da Difusão na Ressonância Magnética da mama—ADC e Kurtosis. Escola Superior de Tecnologia da Saúde de Lisboa (ESTESL). http://hdl.handle.net/10400.21/1728. Accessed 20 Setembro 2018
19. Wu D, Li G, Zhang J et al (2014) Characterization of breast tumors using diffusion kurtosis imaging (DKI). PLoS ONE 9:e113240. https://doi.org/10.1371/journal.pone.0113240
20. Nogueira L, Brandão S, Matos E et al (2014) Application of the diffusion kurtosis model for the study of breast lesions. Eur Radiol 24:1197–1203. https://doi.org/10.1007/s00330-014-3146-5
21. Bickelhaupt S, Jaeger PF, Laun FB et al (2018) Radiomics based on adapted diffusion kurtosis imaging helps to clarify most mammographic findings suspicious for cancer. Radiology. https://doi.org/10.1148/radiol.2017170273
22. Sun K, Chen X, Chai W et al (2015) Breast cancer: diffusion kurtosis MR imaging—diagnostic accuracy and correlation with clinical-pathologic factors. Radiology 277:46–55. https://doi.org/10.1148/radiol.15141625
23. Christou A, Ghiatas A, Priovolos D et al (2017) Accuracy of diffusion kurtosis imaging in characterization of breast lesions. Br J Radiol 90:20160873. https://doi.org/10.1259/bjr.20160873
24. Huang Y, Lin Y, Hu W et al (2018) Diffusion kurtosis at 3.0T as an in vivo imaging marker for breast cancer characterization: correlation with prognostic factors. J Magn Reson Imaging. https://doi.org/10.1002/jmri.26249
25. Woodhams R, Ramadan S, Stanwell P et al (2011) Diffusion-weighted imaging of the breast: principles and clinical applications. RadioGraphics 31:1059–1084. https://doi.org/10.1148/rg.314105160
26. Le Bihan D (2013) Apparent diffusion coefficient and beyond: what diffusion MR imaging can tell us about tissue structure. Radiology 268:318–322. https://doi.org/10.1148/radiol.13130420
27. Partridge SC, McDonald ES (2013) Diffusion weighted MRI of the breast: protocol optimization, guidelines for interpretation, and potential clinical applications. Magn Reson Imaging Clin N Am 21:601–624. https://doi.org/10.1016/j.mric.2013.04.007
28. Poot DHJ, den Dekker AJ, Achten E et al (2010) Optimal experimental design for diffusion kurtosis imaging. IEEE Trans Med Imaging 29:819–829. https://doi.org/10.1109/TMI.2009.2037915
29. Chuhutin A, Hansen B, Jespersen SN (2017) Precision and accuracy of diffusion kurtosis estimation and the influence of b-value selection. NMR Biomed 30:1–14. https://doi.org/10.1002/nbm.3777
30. Padhani AR, Liu G, Mu-Koh D et al (2009) Diffusion-weighted magnetic resonance imaging as a cancer biomarker: consensus and recommendations. Neoplasia 11:102–125. https://doi.org/10.1593/neo.81328
31. Fukunaga I, Hori M, Masutani Y et al (2013) Effects of diffusional kurtosis imaging parameters on diffusion quantification. Radiol Phys Technol 6:343–348. https://doi.org/10.1007/s12194-013-0206-5
32. Koh DM, Collins DJ, Orton MR (2011) Intravoxel incoherent motion in body diffusion-weighted MRI: reality and challenges. Am J Roentgenol 196:1351–1361. https://doi.org/10.2214/AJR.10.5515
33. Chou M-C, Ko C-W, Chiu Y-H et al (2017) Effects of B value on quantification of rapid diffusion kurtosis imaging in normal and acute ischemic brain tissues. J Comput Assist Tomogr 41:868–876. https://doi.org/10.1097/RCT.0000000000000621
34. Yokosawa S, Sasaki M, Bito Y et al (2015) Optimization of scan parameters to reduce acquisition time for diffusion kurtosis imaging at 1.5 T. Magn Reson Med Sci 15:41–48. https://doi.org/10.2463/mrms.2014-0139
35. Mazzoni LN, Lucarini S, Chiti S et al (2014) Diffusion-weighted signal models in healthy and cancerous peripheral prostate tissues: comparison of outcomes obtained at different b-values. J Magn Reson Imaging 39:512–518. https://doi.org/10.1002/jmri.24184
36. Merisaari H, Toivonen J, Pesola M et al (2015) Diffusion-weighted imaging of prostate cancer: effect of b-value distribution on repeatability and cancer characterization. Magn Reson Imaging 33:1212–1218. https://doi.org/10.1016/j.mri.2015.07.004
37. Merisaari H, Jambor I (2015) Optimization of b-value distribution for four mathematical models of prostate cancer diffusion-weighted imaging using b-values up to 2000 s/mm^2: simulation and repeatability study. Magn Reson Med 73:1954–1969. https://doi.org/10.1002/mrm.25310
38. Association of Breast Surgery at BASO (2009) Surgical guidelines for the management of breast cancer. Eur J Surg Oncol 35:S1–S22. https://doi.org/10.1016/j.ejso.2009.01.008
39. Li T, Yu T, Li L et al (2018) Use of diffusion kurtosis imaging and quantitative dynamic contrast-enhanced MRI for the

differentiation of breast tumors. J Magn Reson Imaging 48:1358–1366. https://doi.org/10.1002/jmri.26059
40. DeLong ER, DeLong DM, Clarke-Pearson DL (1988) Comparing the areas under two or more correlated receiver operating characteristic curves: a nonparametric approach. Biometrics 44:837–845
41. Hu F, Tang W, Sun Y et al (2017) The value of diffusion kurtosis imaging in assessing pathological complete response to neoadjuvant chemoradiation therapy in rectal cancer: a comparison with conventional diffusion-weighted imaging. Oncotarget 8:75597–75606. https://doi.org/10.18632/oncotarget.17491
42. Borlinhas F, Nogueira L, Brandão S, et al (2015) Diffusion kurtosis breast imaging model—which should be the highest b-value? In: ISMRM 24th annual meeting—2015, proceedings of the International Society for Magnetic Resonance, 24. Singapore, p 3017
43. Lu H, Jensen JH, Ramani A, Helpern JA (2006) Three-dimensional characterization of non-gaussian water diffusion in humans using diffusion kurtosis imaging. NMR Biomed 19:236–247. https://doi.org/10.1002/nbm.1020
44. Partridge SC, Nissan N, Rahbar H et al (2017) Diffusion-weighted breast MRI: clinical applications and emerging techniques. J Magn Reson Imaging 45:337–355. https://doi.org/10.1002/jmri.25479